International Journal of Mass Spectrometry 303 (2011) 147–153

Contents lists available at ScienceDirect

International Journal of Mass Spectrometry

journal homepage: www.elsevier.com/locate/ijms

Electron ionization of hydrogen sulfide

Kevin M. Douglas, Stephen D. Price*

Department of Chemistry, University College London, 20 Gordon Street, London WC1H 0AJ, UK

ARTICLE INFO

Article history:
Received 9 December 2010
Received in revised form 19 January 2011
Accepted 20 January 2011
Available online 2 February 2011

Keywords:
Electron ionization
Partial ionization cross sections
Hydrogen sulfide
Dication
Multiple ionization
Single ionization

ABSTRACT

Precursor-specific relative partial ionization cross sections, for all the different fragment ions formed by electron ionization of hydrogen sulfide, have been measured using time-of-flight mass spectrometry coupled with a two-dimensional ion coincidence technique. Relative cross sections are reported for ionizing energies from 30 to 200 eV. These cross sections allow the contribution from single, double and triple ionization to the individual fragment ion yields, following ionization of hydrogen sulfide, to be quantified. To compare our data with the literature we reduce our precursor-specific cross sections, by summing them for each fragment ion, to generate relative partial ionization cross sections. Following this data reduction, good agreement is found between our data and one set of recently published absolute partial ionization cross sections, but discrepancies are observed with another set of recently published data. Our analysis shows that the contribution of double ionization to the total ion yield reaches a maximum of 20% at 100 eV. Given the lack of available information on the fate of the excited electronic states of H_2S^{2+}, we have extracted kinetic energy releases for the various dicationic fragmentation channels from our coincidence data. From these kinetic energy releases, estimates of the energies of the electronic states of H_2S^{2+} which are responsible for the different fragmentation channels can be made. These estimates, in comparison with other data on the electronic states of H_2S^{2+}, reveal the population of excited states of H_2S^{2+} at electron energies above 50 eV. At ionizing electron energies above 50 eV, a significant proportion of the major dissociation channels of H_2S^{2+} appear to involve the population of excited electronic states.

1. Introduction

Hydrogen sulfide (H_2S) is a minor constituent of the Earth's atmosphere, and occurs in volcanic and natural gases [1]. Hydrogen sulfide has also been detected in extra-terrestrial environments: interstellar clouds [2,3], comets [4] and planetary atmospheres [5]. To model the role of hydrogen sulfide in these energized environments requires, amongst other factors, a reliable quantification of the consequences of electron-H_2S collisions. This paper describes a series of experiments to determine, for the first time, the *precursor-specific* relative partial ionization cross sections (PICS) following electron ionization of H_2S. Precursor-specific PICS quantify the contribution of different levels of ionization (single, double, triple, ...) to the yield of the fragment ions formed following electron-H_2S collisions. Such precursor-specific cross sections reveal the contribution of different levels of ionization to the more commonly measured PICS [6]. These precursor-specific cross sections provide the most complete picture to date of the consequences of the ionization of H_2S at electron energies from 30 to 200 eV. In addition, the coincidence technique we use to measure our cross sections allows us to probe the energies and fragmentation dynamics of the electronic states of H_2S^{2+}. Particular attention is paid to the dissociation of excited electronic states of H_2S^{2+}, the fate of which has not been well-characterized to date.

A range of experimental techniques have been used to study the ionization of hydrogen sulfide, employing both electron ionization and photoionization. Considering electron ionization, the technique employed in this study, absolute total cross sections following electron ionization have been measured by Belic and Kurepa [7]. Absolute PICS have also been measured by Rao and Srivastava [8], using a time-of-flight (TOF) and a quadrupole mass spectrometer (QMS) in the energy range 0–1000 eV, and by Lindsay et al. [9] in the energy range 16–1000 eV using a time-of-flight mass spectrometer (TOFMS) coupled with a position sensitive detector. The electron ionization of hydrogen sulfide has also been investigated theoretically [10,11].

Experimentally, Lindsay et al. [9] have demonstrated the efficient collection of all ion fragments in their PICS measurements, irrespective of their kinetic energy; an important consideration for determining accurate PICS [9]. However, in the data of Lindsay et al. [9] ion collection efficiency comes at the expense of mass resolution, meaning that their data are reported for groups of ions with similar masses, rather than for individual ion fragments. In a step forward, the mass resolution of our data allows unambiguous identification of all the different fragment ions formed following electron-H_2S collisions.

* Corresponding author. Tel.: +44 20 7679 4606; fax: +44 20 7679 7463.
E-mail address: s.d.price@ucl.ac.uk (S.D. Price).

1387-3806/$ – see front matter © 2011 Elsevier B.V. All rights reserved.
doi:10.1016/j.ijms.2011.01.023

Over the electron energy range investigated in this study (30–200 eV) multiple ionization, particularly double ionization, of H_2S can contribute significantly to the ion yield. Several previous studies have probed the double photoionization of hydrogen sulfide. Initial studies of the fragmentation of H_2S^{2+} were made using an ion coincidence technique [12]. Later, employing threshold photoelectrons coincidence (TPEsCO) and photoelectron–photoion–photoion coincidence (PEPIPICO) techniques, Eland et al. [13,14] investigated the double ionization of H_2S in the energy range 28–48 eV and reported kinetic energy releases for some of the major charge separation channels. The ground and several excited electronic states of H_2S^{2+} have also been probed by Cesar et al. [15] using Auger spectroscopy, computational chemistry and double charge transfer experiments.

In the present study we investigate electron ionization of H_2S in the energy range 30–200 eV using TOF mass spectrometry coupled with a two-dimensional (2D) ion coincidence technique. This experimental method allows single product ions, ion pairs and ion triples, formed following electron ionization of H_2S, to be detected, identified and quantified. From this data we extract precursor-specific relative PICS $\sigma_n[X^{m+}]$ ($n = 1$–3) for all the fragment ions observed. As described above, these precursor-specific cross sections quantify the contribution to individual fragment ion yields from each level of ionization (single $n = 1$, double $n = 2$ and triple $n = 3$). For example, $\sigma_1[S^+]$ quantifies the yield of S^+ ions produced from the fragmentation of singly ionized H_2S. Likewise, $\sigma_2[S^+]$ and $\sigma_3[S^+]$ quantify the yield of S^+ ions produced from the fragmentation of doubly and triply ionized H_2S respectively. To the best of our knowledge these measurements represent the first complete description of the consequences of the single and multiple ionization of H_2S at electron energies below 200 eV. We show, by summation of the different precursor-specific PICS for the different fragment ions, that our precursor-specific data is consistent with the PICS measured by Lindsay et al. [9] for groups of ions with similar masses. In addition, our 2D ion coincidence technique shows that population of the excited states of H_2S^{2+} provides the dominant route to ion pair formation at electron energies between 50 and 100 eV.

2. Experimental

2.1. Apparatus

The apparatus employed in the current investigation has been described before in the literature [16–18]. The experiment couples pulsed electron ionization with a TOFMS of a standard Wiley and McLaren [19] design. The experiment is controlled by a pulse generator running at 50 kHz, which pulses an electron gun and the repeller plate of the TOFMS, and starts the data collection electronics. The pulsed beam of ionizing electrons, with a pulse duration of approximately 30 ns, enters the source region of the TOFMS perpendicular to its main axis. The energy spread of the electron beam is estimated to be 0.5 eV at full width half-maximum [20]. A hypodermic needle is used to create a continuous effusive jet of H_2S in the source region of the TOFMS. This jet is crossed by the electron pulses. Following each ionizing pulse of electrons, the repeller plate is pulsed from 0 to +400 V. This electric field extracts any ions formed by the electron–molecule interactions from the source region of the TOFMS into a second electric field. This second electric field further accelerates the ions into a field-free drift tube. At the end of the drift tube the ions impinge upon a multichannel plate detector (MCP). Signals from the MCP are recorded as ion arrival times by a time to digital converter (TDC) capable of counting multiple stop signals for a single start pulse. The resulting ion flight times from the TDC are accumulated in a memory module and periodically transferred to a PC. The arrival times of single ions, pairs of ions and three ions (triples) at the MCP detector, following a single pulse of electrons, are recorded and used to determine the cross sections of interest, as described below. The hydrogen sulfide gas used was a commercial sample of ≥99.5% purity.

2.2. Experimental conditions

The pressure inside the TOFMS was typically of the order 1×10^{-6} Torr for all experiments, as measured by an ion gauge. Using this low target gas pressure, together with low electron fluxes, ensures that on average there is considerably less than one ionization event per ionizing electron pulse. These conditions significantly reduce the number of 'false coincidences' in our spectra, coincidences which arise when two or more ions from separate ionization events are detected following a single pulse of the repeller plate. In extracting quantitative data from our experiment, we must ensure that no mass or energy discrimination effects are occurring. As described in a recent publication [17], a set of preliminary experiments allows us to identify a range of experimental conditions in which such mass and energy discrimination effects do not influence the ion yields we measure. Under the voltage conditions used in our experiment, ions with a translational energy component of less than 10 eV perpendicular to the TOF axis will reach the detector. As the total kinetic energy release (KER) from a dication dissociation is commonly less than 9 eV [12], conditions in our apparatus are optimized to collect the vast majority of ions formed by multiple ionization. In fact, any loses of energetic ions from multiple ionization can be evaluated and corrected via the shape of the coincidence signals [17,20]. We are, however, unable to quantify any losses of energetic ions with translational energies greater than 10 eV formed from dissociative single ionization. Such losses are expected to be small, as shown by the excellent agreement between the previous cross sections produced from our experiment [16–18,21,22] and literature values from experiments that unequivocally demonstrate the efficient collection all of highly energetic ions.

2.3. Data reduction

Events in which only one ion is detected following a pulse of ionizing electrons are termed 'singles', and their TOFs are histogrammed to produce a 'singles' mass spectrum (Fig. 1). The relative ion intensities ($I_1[X^+]$ for monocations, $I_2[X^{2+}]$ for dications, and if present, $I_3[X^{3+}]$ for trications) in the singles spectra are then extracted by summing the counts in each peak, after applying a small correction to account for the non-zero baseline which arises due to stray ions. As described before, additional corrections are also made to the intensities of the H^+, H_2^+, S^{2+}, H_2S^{2+} and S^+ peaks, due to ions arising from residual air and water in the apparatus [21,22]. Such residual gas signals are the result of the low target gas pressures employed in the experiment to minimise false coincidences. Contributions to the raw ion intensities from these background gases were typically much less then 1% for the H^+, H_2^+ and S^+ peaks and approximately 10% for the very small S^{2+} and H_2S^{2+} peaks (Table 1).

Events in which two or three ions are detected per ionizing pulse are termed 'pairs' and 'triples' respectively. Given the very low rate of ion triples we measure, and that those triples clearly result from dissociation of H_2S^{3+}, contributions to our spectra from quadruple ionization are neglected in this study. The pairs data is quantified by plotting *pairs spectra*, two-dimensional histograms of the flight times of both ions (t_1 versus t_2). Individual decay channels of multiply charged ions appear as distinct peaks in such spectra [23]. The relative intensities of these pairs of ions are determined by summing the counts in each peak, and the count of a given fragment

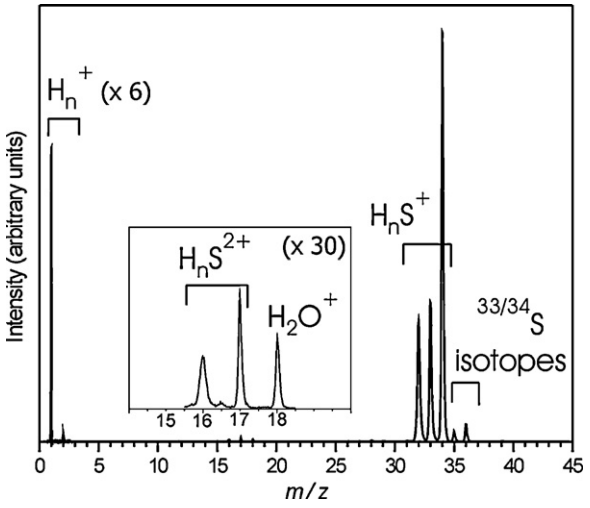

Fig. 1. Typical raw mass spectrum (singles spectrum) of hydrogen sulfide, recorded following ionization by 200 eV electrons. Such raw mass spectra are processed, as described in the text, to remove any contribution from ionization of background gases (e.g., H_2O) and yield the precursor-specific cross sections. The cross sections and isotopic abundances clearly show that the peaks in the expanded region (m/z = 16–17) are dominated by the ions $H_n{}^{32}S^{2+}$ (n = 0–2).

ion in the pairs spectrum, $P_2[X^+]$ and $P_3[X^{m+}]$, are then obtained by summing the counts in all appropriate peaks involving the ion X^+. As discussed in detail before [17,18], $P_3[X^{m+}]$ involves the counts from peaks in the pairs spectrum which must arise from triple ionization, involving a dication and a monocation, such as $S^{++} + H^+$. The values of $P_2[X^+]$ involve the counts from peaks in the pairs spectrum involving pairs of monocations, such as S^+ and H^+. These pairs of monocations can arise from double ionization, or from triple ionization if one of the fragment ions is not detected.

The triples data is quantified in a similar way to the pairs data. First the TOF range of a particular ion is selected, and all ion triples with an ion falling into this range are extracted. The remaining two TOFs are then plotted as a pairs spectrum, and the intensity of each ion triple peak found by summing the number of counts in the peak. The contribution of a fragment ion to the triples spectrum, $T[X^+]$, is then obtained by summing the counts of all appropriate peaks involving the ion X^+. In practice, the only true triple event we detect following electron ionization of H_2S is $S^+ + H^+ + H^+$, justifying our neglect of quadruple and higher levels of ionization.

Although our experimental conditions are maintained so that false coincidences are kept to a minimum, it is still necessary to correct the pairs and triples spectra for the few false coincidences that do occur. The number of false coincidences are evaluated manually for each peak, using the autocorrelation of the singles spectrum [17]. As with the singles spectrum, additional corrections are also made to some of the ion pairs for ion contributions arising from residual water in the apparatus. Contributions from these residual gases to the counts of the weak $H^+ + H^+$ and $S^{2+} + H^+$ ion pair peaks were typically less than 1% and 10% respectively.

Table 1
Raw counts, and counts corrected for the contribution of dissociative ionization of H_2O, for the signals at m/z = 16–18 from a representative mass spectrum recorded at an electron energy of 200 eV. As described in the text, after the displayed correction for the contribution from dissociative ionization of H_2O, the peak counts are then corrected for the isotopic abundances of sulfur.

Major ion	$^{32}S^{2+}$	$H^{32}S^{2+}$	$H_2{}^{32}S^{2+}$	H_2O^+
Peak m/z	16	16.5	17	18
Raw counts	8933	839	9984	4379
Corrected counts	8659	839	8629	0

In our singles and pairs spectra, we are unable to distinguish between the isotopologues of a number of sulphur containing ions which occur at the same mass in the singles spectrum; for example, $H_2{}^{32}S^+$, $H^{33}S^+$ and $^{34}S^+$. Thus, the measured ion intensities were corrected numerically for isotopic speciation using the natural isotopic distribution ^{32}S:^{33}S:^{34}S (95.0%:0.8%:4.2%).

In our experimental arrangement, due to the 'deadtime' of the discrimination circuitry, an ion-pair will not be detected if the second ion arrives at the detector within 32 ns of the first. This results in a 'dead region' in the pairs spectrum affecting the $H^+ + H^+$ peak. An estimate of the losses within this dead region can be made by first plotting the time-of-flight difference (ΔTOF) between pairs of ions making up the visible part of the affected pairs peak. Extrapolation of this ΔTOF plot can then be made, using simple geometry, to quantify the counts lost in the dead region [24].

The gradient of the peaks in the pairs spectrum, which yields the correlation of the fragment ions' momenta, can provide information on the mechanism of a given three-body dissociation reactions of multiply charged ions [23,25]. Using a Monte-Carlo simulation to model the form of the ΔTOF plots for an individual peak in the pairs spectrum yields the KER of a given dissociation channel [25]. We can estimate the energy of the H_2S^{2+} precursor state from which the ion pair was formed, by adding the KER to the asymptotic energy of the fragmentation products.

From the recorded intensities of fragment ions in the singles, pairs and triples spectra, together with a value for the ion detection efficiency f_i of the apparatus, the $\sigma_n[X^{m+}]$ values can be evaluated. Values of the more commonly encountered relative PICS $\sigma_r[X^{m+}]$ can also be determined for comparison with existing measurements, effectively by summing the precursor-specific PICS for a given ion. One example of the sets of equations used to calculate relative and precursor-specific relative PICS are given below (Eqs. (1) and (2)). The value of f_i accounts for the non-unit transmission efficiency of the grids that define the electric fields in our apparatus, and also the performance of the detector and electronics. To determine f_i separate experiments are carried out in which the intensities of single ions and ion pairs formed following electron ionization of CF_4 are recorded [17]. The recorded experimental intensities are then compared to those extracted from published data [24,26,27], allowing a value of f_i to be calculated. For a full description of the data reduction procedure, including the determination of f_i and the algorithms used to calculate relative and precursor-specific relative PICS, readers are directed to previous publications [17,18,28,29].

$$\sigma_1[X^+] = \frac{I[X^+] - ((1-f_i)/f_i)(P_2[X^+] + P_3[X^+]) + ((1-f_i)^2/f_i^2)T[X^+]}{I[\text{parent}^+]} \quad (1)$$

$$\sigma_r[X^+] = \sum_{n-1}^{3} \sigma_n[X^+] = \frac{I[X^+] + P_2[X^+] + P_3[X^+] + T[X^+]}{I[\text{parent}]^+} \quad (2)$$

3. Results

Mass and coincidence spectra of hydrogen sulfide have been recorded at ionizing electron energies in the range 30–200 eV. A representative raw mass spectrum can be seen in Fig. 1. These spectra were processed, as described above, to yield precursor-specific relative PICS $\sigma_n[X^{m+}]$ for the formation of all fragment ions observed: HS^+, S^+, H_2S^{2+}, HS^{2+}, S^{2+}, $H_2{}^+$ and H^+. In addition, as described above, for comparison with previous work, relative PICS $\sigma_r[X^{m+}]$ were also derived from our dataset. These $\sigma_r[X^{m+}]$ and $\sigma_n[X^{m+}]$ (n = 1–3) values are expressed relative to the H_2S^+ ion yield, and are displayed as a function of electron energy in Figs. 2 and 3 and given numerically in the Supplementary information (Tables S1 and S2). These relative values can be readily

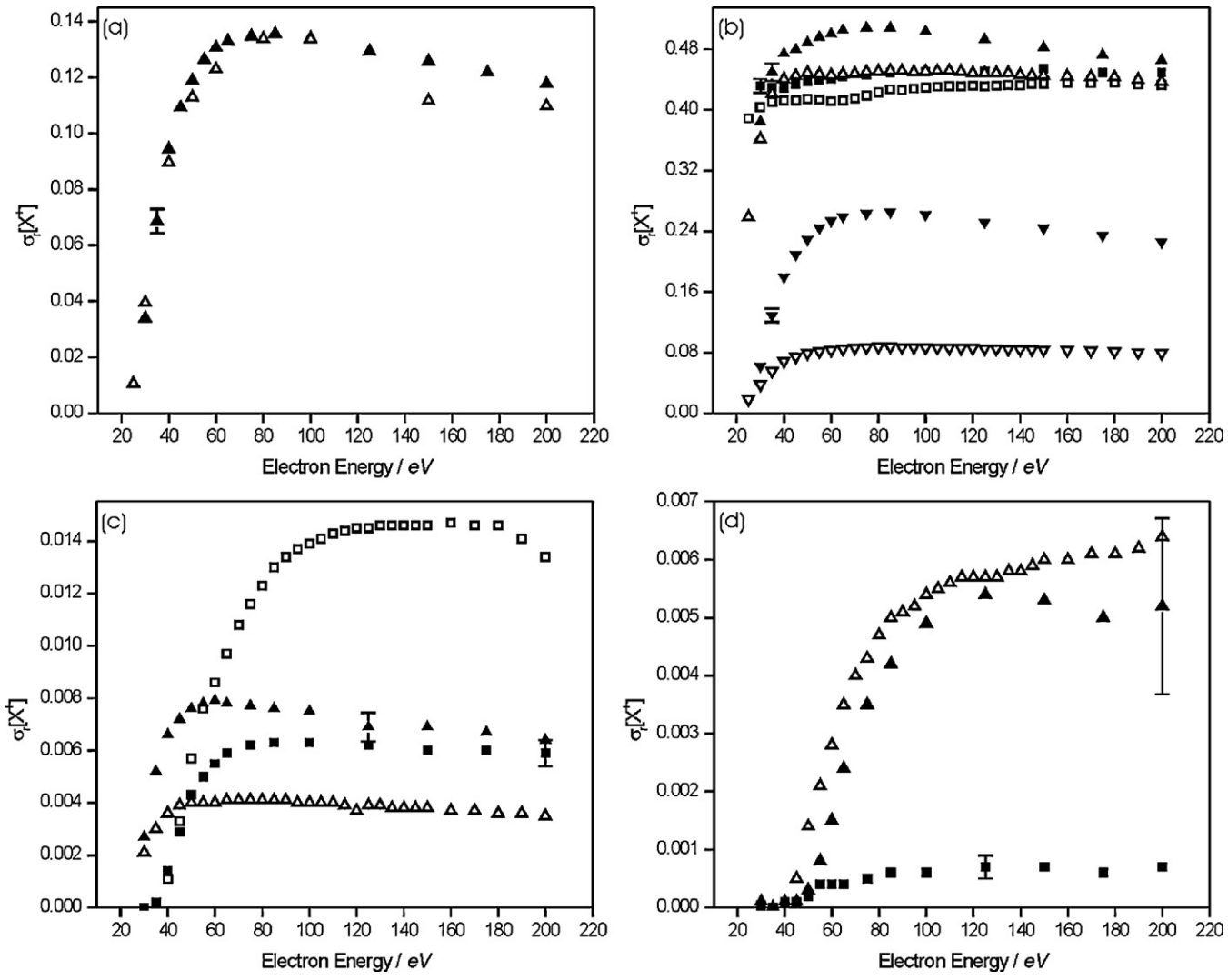

Fig. 2. Relative PICS $\sigma_r[X^{m+}]$ for forming (a) H^+ following electron ionization of H_2S, relative to the summed cross sections for forming the group of ions H_nS^+, (b) S^+ (▲), HS^+ (■), and H^+ (▼), (c) H_2^+ (▲), H_2S^{2+} (■) and (d) S^{2+} (▲) and H_2S^{2+} (■) following electron ionization of H_2S relative to the cross section for forming the parent ion H_2S^+. Where available the corresponding relative PICS from the data of Lindsay et al. (graph (a)) and Rao and Srivastava (graphs (b–d)) are also shown as open symbols. The representative error bars show two standard deviations of four separate determinations.

placed on an absolute scale, using the measurements of the total ionization cross section [7].

In the coincidence spectra, we observe four ion pairs generated predominantly by the dissociation of H_2S^{2+} ($H^+ + H^+$, $S^+ + H^+$, $S^+ + H_2^+$ and $HS^+ + H^+$) and two ion pairs clearly formed from the dissociation of H_2S^{3+}: $S^{2+} + H^+$, $HS^{2+} + H^+$. Above the double ionization threshold, the ion pair yield is dominated (>90%) by the formation of $SH^+ + H^+$ and $S^+ + H^+$, with the former channel the most intense at electron energies up to 65 eV and the latter channel more intense above that energy. A similar dominance of these two ion pair decay channels is observed for H_2S^{2+} formed by photoionization [13]. As noted above, we also observe one ion triple channel from the dissociation of H_2S^{3+} ($H^+ + H^+ + S^+$). The overall contributions from single, double and triple ionization to the total ion yield can be evaluated from our data. Such an analysis shows that as the ionizing electron energy is increased from 30 to 200 eV the relative contribution to the ion yield from single ionization broadly drops (50 eV: 89%, 100 eV: 80%, 200 eV: 82%). This drop coinciding with an increase in the contribution to the ion yield from double ionization (50 eV: 11%, 100 eV: 20%, 200 eV: 18%) and triple ionization. However, the contribution from triple ionization is negligible below 85 eV and very small (0.1–0.3%) above 85 eV.

As discussed above, a value for the ion detection efficiency f_i is required to enable us to derive $\sigma_n[X^{m+}]$ values. Measurement of f_i for our apparatus, using the methodology described above, resulted in a value of 0.26 ± 0.01, in good agreement with previous determinations [16–18,20,30].

4. Discussion

4.1. Precursor-specific relative partial ionization cross sections

The values of σ_1, σ_2 and σ_3 for the formation of fragment ions formed following election ionization of H_2S are displayed in Fig. 3 and given numerically in the Supplementary information (Table S2). Our data show dissociative single ionization makes the major contribution to the yields of all the singly charged fragment ions (H^+, H_2^+, S^+ and HS^+), but double ionization also contributes significantly. Due to the small number of counts present in the triple channel $H^+ + H^+ + S^+$, the only channel that contributes to $\sigma_3[S^+]$, there is a significant uncertainty associated with these values. However, the general trend of the $\sigma_3[S^+]$ values can be seen to be in line with other $\sigma_3[X^{m+}]$ values.

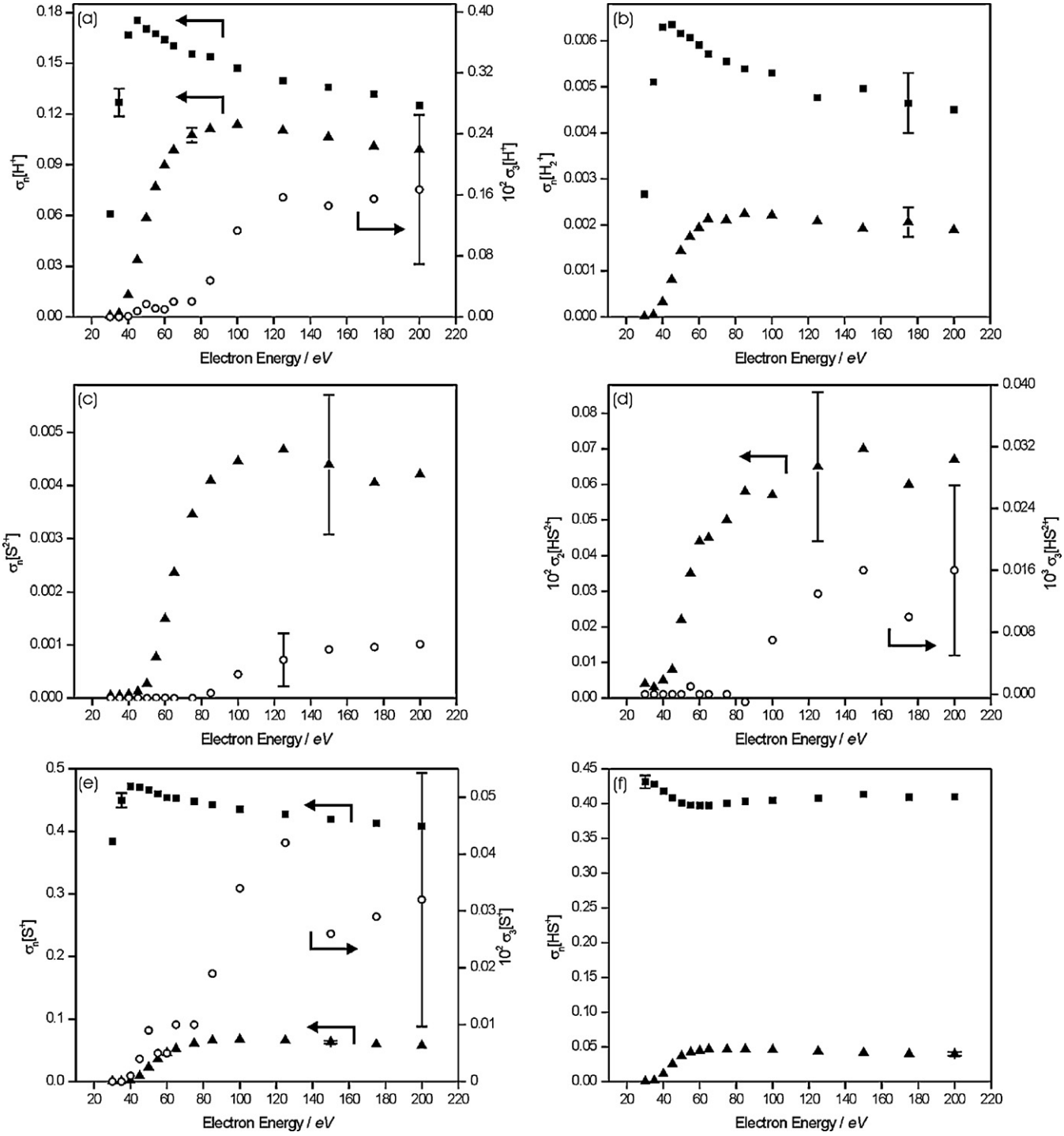

Fig. 3. Relative precursor-specific PICS for forming (a) H^+, (b) H_2^+, (c) S^{2+}, (d) HS^{2+}, (e) S^+ and (f) HS^+ fragment ions via single (■), double (▲) and triple (○) ionization, following electron ionization of H_2S, relative to the cross-section for forming the parent ion H_2S^+. The representative error bars shows two standard deviations of four separate determinations, except for $\sigma_3[S^+]$ (panel (e), (○)), for which only one standard deviation is given.

In comparison with H_2O, where the maximum contribution of double ionization to the ion yield is 5% [22], the presence of a sulphur atom in H_2S, an atom from the second row of the periodic table with associated greater electron correlation, raises the maximum contribution of double ionization to the ion yield to 20%. Indeed, from our recent data there is a broad linear correlation ($r = 0.8$) between the maximum contribution of double ionization to the ion yield and the number of electrons in the molecule: CH_4 (12%) [31], C_2H_2 (11%) [17], HCl (11%) [20], CH_3OH (20%) [16], CO_2 (17%) [21], and $SiCl_4$ (35%) [29].

4.2. Relative partial ionization cross sections

The values of $\sigma_r[X^{m+}]$ we have derived from our data are displayed in Fig. 2 and given numerically in the Supplementary information (Table S1). Given that this paper presents the first measurement of the precursor-specific PICS, it is only by constructing the relative PICS from our data that we can compare our results with previous work. Our relative PICS are compared with values derived from the data of Rao and Srivastava [8] (Fig. 2b–d). To enable a direct comparison with the results of Lindsay et al. [9] who report PICS for

Table 2
Kinetic energy releases (KERs, uncertainty ± 0.6 eV unless stated), and corresponding precursor state energies *P*, for selected dissociation reactions of H_2S^{2+}. The weightings of the KERs are listed, together with an average KER to facilitate a direct comparison with literature. The electron energy of the spectral data used to determine the KERs are also given. The energies of the dissociation asymptotes, relative to the ground state of H_2S, involved in the determination of *P* are listed. Unless indicated, such asymptotes correspond to the formation of ground state products.

Ion pair	Electron energy (eV)	KER (eV)	Weight (%)	Average KER		Asymptote [36] (eV)	*P* (eV)
				This work	Refs. [12,13]		
$HS^+ + H^+$	55	2.2	25	6.0	5.4 ± 0.4	29.1	31.3[a]
		5.8	50			27.9	33.7
		10.3	25				38.2
$S^+ + H_2^+$	100	3.5	50	5.1	5.2 ± 0.5	28.9	32.4
		5.6	35				34.5
		9.5 ± 1.0	15				38.4
$S^+ + H^+$	55	2.6	30	6.2	5.5	31.6	34.2
		6.0	40				37.6
		10.0	30				41.6

[a] This precursor state and asymptote correspond to the formation of the first excited singlet state of HS^+. See text for details.

H^+ and the group of ions H_nS^+ (n = 0–2), we have also calculated the relative PICS for H^+ relative to the summed cross section for the H_nS^+ group of ions, as shown in Fig. 2a.

Comparison of our $\sigma_r[H^+]$ values to those derived from the work of Lindsay et al. [9] in which the efficient collection of all ion fragments with considerable translational energy was demonstrated, show good agreement at all ionizing electron energies investigated (Fig. 2a). By contrast, there is a significant difference between some of the values of $\sigma_r[X^+]$ we determine and those derived from the data of Rao and Srivastava [8]. Specifically, good agreement is observed for the heavier ion fragments (HS^+ and S^+), and for the fragment ion S^{2+} the $\sigma_r[X^{m+}]$ values agree within mutual error limits, although our values are systematically slightly higher. However, for the lighter ion fragments (H_2^+ and H^+) the values of $\sigma_r[X^+]$ derived in the current work are significantly higher than those of Rao and Srivastava [8]. These differences for H^+ and H_2^+ can be explained by the inefficient collection of translationally energetic ions in this earlier work, as has been discussed before [17,22,32]. Indeed, better agreement is observed comparing our $\sigma_1[X^{m+}]$ values for H^+ and H_2^+ to the $\sigma_r[X^+]$ values derived from the work of Rao and Srivastava [8] indicating the majority of ion losses in this earlier work are from dissociative double or triple ionization. Another significant difference between our data and that of Rao and Srivastava [8] involves the values we obtain for $\sigma_r[H_2S^{2+}]$; here, conversely, our values are about half of that reported in the previous work. A possible explanation for these differences in the values of $\sigma_r[H_2S^{2+}]$ is due to the lifetime of the metastable H_2S^{2+} ion. Specifically, the lifetime of a subset of the H_2S^{2+} ions formed in our electron-molecule collisions is clearly of the order of a few hundred nanoseconds, as readily evidenced by the metastable tail from the $HS^+ + H^+$ peak in the pairs spectrum. In our experiments the flight time of an H_2S^{2+} ion is 1820 ns. If, in the experiments of Rao and Srivastava [8], the H_2S^{2+} ions lived for a significantly shorter time than 1820 ns before their detection then the $\sigma_r[H_2S^{2+}]$ values derived from the data of Rao and Srivastava [8] would be larger than our data.

4.3. Energetics and dissociation of H_2S^{2+}

Often initial information on the electronic states of small molecular dications was provided by detecting the pairs of fragment ions from a dicationic dissociation in coincidence [12,33]. As described above, the kinetic energy releases derived from these coincidence spectra were added the asymptotic energies of the products to provide an estimate of the energy of the electronic state of the dication responsible for the dissociation [17,21,22]. However, new coincidence techniques have generally superseded simple ion coincidence spectrometry for probing the vibronic energy levels of small dications. For H_2S^{2+} electron–electron coincidence studies [14] resolve the first four vibrational levels of the dicationic ground state ($X\ ^1A_1$), accurately determining the energy of the vibronic ground state (31.664 eV) with respect to the ground state of H_2S. However, no resolved structure assignable to higher electronic states is observed. In the light of this lack of data on the fate of the excited states of H_2S^{2+}, although the energies of such states have been probed by Auger and double-charge transfer spectroscopy [15], we feel justified in extracting kinetic energy releases from our coincidence data to see what new information we can derive regarding the fate of the excited states of H_2S^{2+}.

As described above, we extract kinetic energy release distributions for the different fragmentation channels of H_2S^{2+}, by fitting the experimental ΔTOF spectrum [12] with a Monte-Carlo simulation of the dissociation. For each channel we use the data at the lowest electron energy which generates a statistically significant ΔTOF spectrum. For two-body dissociations the Monte Carlo simulation can be directly employed to model the ΔTOF peaks, directly yielding the KER. As can be seen from Table 2, more than one KER value was required to satisfactorily fit the experimental ΔTOF spectra, if the width of the (Gaussian) KER distribution was restricted to realistic values, below 1.5 eV. The H_2S^{2+} precursor state energies derived from these KER measurements should be viewed as lower limits as they neglect any internal energy in the dissociation products. Good agreement is observed between the average of our KER values (Table 2) and the results of Eland et al. [13] and Curtis and Eland [12] recorded following photoionization of hydrogen sulfide.

For the ion pair $HS^+ + H^+$, the lowest H_2S^{2+} precursor state energy we derive is 31.3 ± 0.6 eV, given that [13,34], due to spin correlations, that the ground ($^1A_1$) state of H_2S^{2+} does not dissociate to the ground state products but to $H^+ + HS^+$ ($a^1\Delta$). This precursor state energy is in good agreement with the experimentally determined energy of the ground state of H_2S^{2+} (31.6 eV). However, the ground $^1A_1$ state of H_2S^{2+} is metastable with a barrier of approximately 2 eV to dissociation [34]. Thus it seems clear that this precursor energy must correspond to the population of the dissociative monocation states lying close to the vertical double ionization energy. These states have been implicated in the formation of monocation pairs from H_2S at energies below the double ionization potential [13].

Cesar et al. [15] have presented (their Table VII) the energies of the states of H_2S^{2+} determined from double charge transfer spectroscopy, Auger spectroscopy and theory. Comparing the state energies presented by Cesar et al. [15] with the latest value of the double ionization energy of H_2S [14], it seems clear that for the lower states of H_2S^{2+} the theoretical values of Cesar et al. [15] should be shifted upwards by about 1 eV, whilst the energies determined by double charge transfer experiments should be shifted down in energy by about 1 eV. In the light of this adjustment, the assignment of the $H^+ + HS^+$ precursor state we observe at 33.7 ± 0.6 eV to the second excited state ($^1B_1$) of H_2S^{2+} appears

logical. Population of this precursor state (Table 2) dominates the product flux in the $H^+ + HS^+$ channel. Our assignment implies that curve crossings to other dissociative states allow the $^1B_1$ state of H_2S^{2+} to dissociate to the, nominally spin-forbidden, ground state products.

The final precursor state energy we extract from the $H^+ + HS^+$ energy release spectrum lies at 38.2 eV. The energy of this state agrees well with the first $^1B_2$ excited state of H_2S^{2+} revealed by Cesar et al. [15], recalling that the precursor state energy is a lower limit. However, given that this state lies over 7 eV above the ground state of H_2S^{2+}, where the electronic state density is likely to be high, this assignment should be viewed as tentative.

The two lowest energy precursor states we derive from the KERs (Table 2) in the $S^+ + H_2^+$ channel match well with the energies of the first two excited states of H_2S^{2+}, the $^3B_1$ state lying at 32.6 eV and $^1B_1$ state at 34.1 eV [15]. The highest energy precursor state in the $S^+ + H_2^+$ channel (38.4 ± 0.6 eV) agrees well with the highest energy precursor state in the $H^+ + HS^+$ channel (38.2 eV), which we tentatively assigned to the first $^1B_2$ excited state of H_2S^{2+} [15].

To extract the KER values for the three-body dissociation of H_2S^{2+}, where a neutral H fragment is formed together with S^+ and H^+, the mechanism of the dissociation is first required. As described above, in principle, this mechanistic information can be extracted from the gradient of the peak in the pairs spectrum [12,23]. The gradient of the $S^+ + H^+$ peak in the pairs spectrum indicates [12,23] an initial separation of H_2S^{2+} into $S^+ + H_2^+$, followed by a secondary dissociation of the H_2^+ into $H^+ + H$. The calculated gradient for such a dissociation pathway is −0.50, in good agreement with the observed gradient of −0.52. Using this mechanism, three KERs were required to satisfactorily fit the experimental ΔTOF spectrum (Table 2). The lowest precursor state energy (34.2 eV) corresponding to these KERs (Table 2) agrees well with the energy of the $^1B_1$ state, which we concluded above also dissociates to $H_2^+ + S^+$. Satisfyingly, as discussed above, the slope of the $H^+ + S^+$ peak in the pairs spectrum indicates that this three body reaction proceeds via initial formation of the $H_2^+ + S^+$ ion pair. Thus, it seems clear that the $^1B_1$ state initially dissociates to form $H_2^+ + S^+$ with some of the H_2^+ ions being sufficiently excited to dissociate to $H^+ + H$. Given the state energies of Cesar et al. [15], the $H^+ + S^+$ precursor state at 37.6 eV can be tentatively assigned to the first excited $^1A_1$ state and the state at 41.6 eV to the second excited $^1A_1$ state.

Satisfyingly, our precursor state energies and assignments in the $HS^+ + S^+$ and $H^+ + S^+$ channels agree well with observed threshold energies for energetic H^+ formation, above the double ionization potential, measured by Dunn et al. [35] For the remaining ion pairs observed ($H^+ + H^+$, $SH^{2+} + H^+$ and $S^{2+} + H^+$), at all ionizing electron energies investigated, insufficient counts were available to produce statistically significant KERs.

5. Conclusions

Precursor-specific relative partial ionization cross sections for the fragment ions formed by electron ionization of hydrogen sulfide have been measured using time-of-flight mass spectrometry coupled with a 2D ion coincidence technique. Relative cross sections are reported for ionizing energies from 30 to 200 eV. These cross sections allow the contribution from single, double and triple ionization to the individual fragment ion yields, following ionization of hydrogen sulfide, to be quantified for the first time. To validate our measurements we also present sums of our precursor-specific values, for a given fragment ion, which we can compare with previous measurements of the partial ionization cross sections of H_2S. Good agreement is found between our data and one set of recently published absolute partial ionization cross sections [9]. Conversely, discrepancies are observed with another set of recently published data [8]; discrepancies we attribute to the loss of translationally energetic fragment ions. Our analysis shows that the contribution of double ionization to the total ion yield reaches a maximum of 20% at 100 eV. We have extracted kinetic energy releases for the various dicationic fragmentation channels from our coincidence data. From these kinetic energy releases, estimates of the energies of the electronic states of H_2S^{2+} which are responsible for the different fragmentation channels can be made. These estimates, in comparison with other data on the electronic states of H_2S^{2+}, reveal that at electron energies above 50 eV, the population of excited electronic states of H_2S^{2+} are major pathways to charge separation.

Acknowledgements

We acknowledge the support of the Royal Society, EPSRC and UCL for this work.

Appendix A. Supplementary data

Supplementary data associated with this article can be found, in the online version, at doi:10.1016/j.ijms.2011.01.023.

References

[1] C.H. Lin, I.F. Mao, P.H. Tsai, H.Y. Chuang, Y.J. Chen, M.L. Chen, Environ. Res. 110 (2010) 536, doi:10.1016/j.envres.2010.05.009.
[2] P. Thaddeus, R.W. Wilson, M.L. Kutner, K.B. Jefferts, A.A. Penzias, Astrophys. J. 176 (1972) L73.
[3] Y.C. Minh, W.M. Irvine, L.M. Ziurys, Astrophys. J. 345 (1989) L63.
[4] J. Crovisier, D. Despois, D. Bockeleemorvan, P. Colom, G. Paubert, Icarus 93 (1991) 246.
[5] V.A. Krasnopolsky, Icarus 197 (2008) 377, doi:10.1016/j.icarus.2008.05.020.
[6] T.D. Märk, G.H. Dunn, in: T.D. Märk, G.H. Dunn (Eds.), Electron Impact Ionization, Springer-Verlag, New York, 1985, p. 137.
[7] D.S.M. Belic, V. Kurepa, Fizika (Zagreb) 17 (1985) 117.
[8] M.V.V.S. Rao, S.K. Srivastava, J. Geophys. Res. 98 (1993) 13137.
[9] B.G. Lindsay, R. Rejoub, R.F. Stebbings, J. Chem. Phys. 118 (2003) 5894, doi:10.1063/1.1556613.
[10] S.P. Khare, W.J. Meath, J. Phys. B 20 (1987) 2101.
[11] Y.K. Kim, W. Hwang, N.M. Weinberger, M.A. Ali, M.E. Rudd, J. Chem. Phys. 106 (1997) 1026.
[12] D.M. Curtis, J.H.D. Eland, Int. J. Mass Spectrom. Ion Process. 63 (1985) 241.
[13] J.H.D. Eland, P. Lablanquie, M. Lavollee, M. Simon, R.I. Hall, M. Hochlaf, F. Penent, J. Phys. B 30 (1997) 2177.
[14] J.H.D. Eland, Chem. Phys. 294 (2003) 171.
[15] A. Cesar, H. Agren, A.N. Debrito, S. Svensson, L. Karlsson, M.P. Keane, B. Wannberg, P. Baltzer, P.G. Fournier, J. Fournier, J. Chem. Phys. 93 (1990) 918.
[16] K.M. Douglas, S.D. Price, J. Chem. Phys. 131 (2009) 224305.
[17] S.J. King, S.D. Price, J. Chem. Phys. 127 (2007) 174307.
[18] N.A. Love, S.D. Price, Phys. Chem. Chem. Phys. 6 (2004) 4558.
[19] W.C. Wiley, I.H. McLaren, Rev. Sci. Inst. 26 (1955) 1150.
[20] S. Harper, P. Calandra, S.D. Price, Phys. Chem. Chem. Phys. 3 (2001) 741.
[21] S.J. King, S.D. Price, Int. J. Mass Spectrom. 272 (2008) 154.
[22] S.J. King, S.D. Price, Int. J. Mass Spectrom. 277 (2008) 84.
[23] J.H.D. Eland, Mol. Phys. 61 (1987) 725.
[24] M.R. Bruce, L. Mi, C.R. Sporleder, R.A. Bonham, J. Phys. B 27 (1994) 5773.
[25] J.H.D. Eland, Chem. Phys. Lett. 203 (1993) 353.
[26] M.R. Bruce, R.A. Bonham, Int. J. Mass Spectrom. Ion Process. 123 (1993) 97.
[27] M.R. Bruce, C. Ma, R.A. Bonham, Chem. Phys. Lett. 190 (1992) 285.
[28] M.D. Ward, S.J. King, S.D. Price, J. Chem. Phys. 134 (2011) 024308.
[29] S. King, S.D. Price, J. Chem. Phys., in press, doi:10.1063/1.3532928.
[30] P. Calandra, C.S.S. O'Connor, S.D. Price, J. Chem. Phys. 112 (2000) 10821.
[31] P.Q. Wang, C.R. Vidal, Chem. Phys. 280 (2002) 309.
[32] C.C. Tian, C.R. Vidal, J. Phys. B 31 (1998) 895.
[33] G. Dujardin, S. Leach, O. Dutuit, P.M. Guyon, M. Richardviard, Chem. Phys. 88 (1984) 339.
[34] S.A. Pope, I.H.M. Hillier, F. Guest, Faraday Symp. Chem. Soc. (1984) 109.
[35] K.F. Dunn, R. Browning, M.A. MacDonald, C.R. Browne, C.J. Latimer, J. Phys. B 31 (1998) 4173.
[36] P.J. Linstrom, W.G. Mallard (Eds.), NIST Chemical WebBook, NIST Standard Reference Database Number 69 (National Institute of Standards and Technology, Gaithersburg MD, 20899, 2008).